Phytomedicine Plus 1 (2021) 100135

Contents lists available at ScienceDirect

Phytomedicine Plus

journal homepage: www.sciencedirect.com/journal/phytomedicine-plus

Computational screening of phytochemicals from three medicinal plants as inhibitors of transmembrane protease serine 2 implicated in SARS-CoV-2 infection

Omotayo O. Oyedara [a,b,*], Joseph M. Agbedahunsi [c], Folasade M. Adeyemi [a], Alfredo Juárez-Saldivar [d], Olatomide A. Fadare [e], Charles O. Adetunji [f], Gildardo Rivera [d]

[a] Department of Microbiology, Osun State University, Osogbo, Nigeria
[b] Departamento de Microbiología e Inmunología, Facultad de Ciencias Biológicas, Universidad Autónoma de Nuevo León, San Nicolás de los Garza, Nuevo León, 66455, Mexico
[c] Drug Research and Production Unit, Faculty of Pharmacy, Obafemi Awolowo University, Ile-Ife, Osun State, 220005, Nigeria
[d] Laboratorio de Biotecnología Farmacéutica, Centro de Biotecnología Genómica, Instituto Politécnico Nacional, Reynosa, 88710, México
[e] Department of Chemistry, Obafemi Awolowo University, Ile-Ife
[f] Applied Microbiology, Biotechnology and Nanotechnology Laboratory, Department of Microbiology, Edo State University, Uzairue, Edo State, Nigeria

ARTICLE INFO

Keywords:
Molecular docking
TMPRSS2
SARS-CoV-2
M. oleifera
Phytochemical
ADMET

ABSTRACT

Background: SARS-CoV-2 infection or COVID-19 is a major global public health issue that requires urgent attention in terms of drug development. Transmembrane Protease Serine 2 (TMPRSS2) is a good drug target against SARS-CoV-2 because of the role it plays during the viral entry into the cell. Virtual screening of phytochemicals as potential inhibitors of TMPRSS2 can lead to the discovery of drug candidates for the treatment of COVID-19.

Purpose: The study was designed to screen 132 phytochemicals from three medicinal plants traditionally used as antivirals; *Zingiber officinalis* Roscoe (Zingiberaceae), *Artemisia annua* L. (Asteraceae), and *Moringa oleifera* Lam. (Moringaceae), as potential inhibitors of TMPRSS2 for the purpose of finding therapeutic options to treat COVID-19.

Methods: Homology model of TMPRSS2 was built using the ProMod3 3.1.1 program of the SWISS-MODEL. Binding affinities and interaction between compounds and TMPRSS2 model was examined using molecular docking and molecular dynamics simulation. The drug-likeness and ADMET (absorption, distribution, metabolism, excretion, and toxicity) properties of potential inhibitors of TMPRSS2 were also assessed using admetSAR web tool.

Results: Three compounds, namely, niazirin, quercetin, and moringyne from *M. oleifera* demonstrated better molecular interactions with binding affinities ranging from -7.1 to -8.0 kcal/mol compared to -7.0 kcal/mol obtained for camostat mesylate (a known TMPRSS2 inhibitor), which served as a control. All the three compounds exhibited good drug-like properties by not violating the Lipinski rule of 5. Niazirin and moringyne possessed good ADMET properties and were stable in their interactions with the TMPRSS2 based on the molecular dynamics simulation. However, the ADMET tool predicted the potential hepatotoxic and mutagenic effects of quercetin.

Conclusion: This study demonstrated the potentials of niazirin, quercetin, and moringyne from *M. oleifera*, to inhibit the activities of human TMPRSS2, thus probably being good candidates for further development as new drugs for the treatment or management of COVID-19.

Abbreviations: ADMET, Absorption, distribution, metabolism, excretion and toxicity; BBB, Blood brain barrier; CASTp, Computed atlas of surface topography of proteins; COVID-19, Coronavirus Disease 2019; GMQE, Global quality estimation score; HIA, Human intestinal absorption; HOB, Human oral bioavailability; LD_{50}, Lethal dose 50; QMEAN, Qualitative Model Energy Analysis; SARS-CoV-2, Severe Acute Respiratory Syndrome Coronavirus 2; TMPRSS2, Transmembrane Protease Serine 2; RMSD, Root-mean-square deviation.

* Corresponding author: Department of Microbiology, Osun State University, PMB 4494, Oke Baale, Osogbo, Osun State, Nigeria.
E-mail address: omotayo.oyedara@uniosun.edu.ng (O.O. Oyedara).

https://doi.org/10.1016/j.phyplu.2021.100135
Received 6 May 2021; Received in revised form 20 September 2021; Accepted 27 September 2021
Available online 29 September 2021

Introduction

SARS-CoV-2 is an envelope and a spiked positive-stranded ribonucleic acid (RNA) virus responsible for a severe acute respiratory syndrome (SARS) termed Coronavirus Disease 2019 (COVID-19), with some symptoms such as cough, sore throat, fever, pneumonia, alveolar damage, and inflammatory responses in the airways ultimately leading to severe respiratory failure. SARS-CoV-2 possesses a 30 kb genome encoding non-structural proteins (viral proteases, transcription, and replication proteins) and structural proteins (nucleocapsid, membrane, envelope, and spike). The spike is a glycosylated protein that plays a significant role during SARS-CoV-2 infection. It recognizes and binds to a receptor known as angiotensin-converting enzyme 2 (ACE-2) on the host cell surface prior to the virus entry into host cells via receptor mediated endocytosis (Pandey et al. 2020). Furthermore, the successful internalization of SARS-CoV-2 into the human host cell is a function of the presence of a cellular protease Transmembrane Protease Serine 2 (TMPRSS2), which primes the glycosylated spike protein to allow the virus fuse with the host membrane (Hoffmann et al. 2020).

The critical role TMPRSS2 plays during SARS-CoV-2 infection makes it a good target for drug development in the treatment of COVID-19 disease or amelioration of conditions of patients infected with the SARS-CoV-2 virus. Although several research efforts have been committed to the discovery of drugs to combat COVID-19, there has been no success in the development of approved antiviral drugs. The inhibitory activities of compounds and drugs against TMPRSS2 have been reported (Vivek-Ananth et al. 2020). For instance, clinically approved drugs such as camostat mesylate and nafamostat have been reported as potent inhibitors of TMPRSS2 (McKee et al. 2020). Recent *in silico* studies have identified several phytochemicals from different plants as potential inhibitors of TMPRSS2. Pooja et al. (2021) identified columbin and jatrorrhizine from *Tinospora cardifolia* (Willd.) Miers (Menispermaceae), baicalein from *Scutellaria baicalensis* Georgi (Lamiaceae), proanthocynidine A2 from *Litchi chinensis* Sonn. (Sapindaceae), and myricetin from *Torreya nucifera* (L.) Siebold & Zucc. (Taxaceae) as potential TMPRSS2 inhibitors. Furthermore, the inhibitory potentials of antiviral phytochemicals, including bisdemethoxycurcumin, carvacrol, and thymol from common Indian spices, namely *Trachyspermum ammi* (L.) Sprague (Apiaceae), *Curcuma longa* L. (Zingiberaceae), and *Nigella sativa* L. (Ranunculaceae) against TMPRSS2 were reported by Yadav et al. (2021).

Plant-based natural products have been recognised as an excellent source of novel drugs. Different plant species have been converted into pharmacological drugs which have been applied for successful treatment of several human ailments such as malaria, hypertension, and cancer. Small molecules derived from natural products are not only readily abundant, but they have also been reported to be orally active according to the Lipinski rule of compound druggability (Benet et al. 2016). The plants of interest in this study include *Zingiber officinalis* Roscoe (Zingiberaceae), *Artemisia annua* L. (Asteraceae), and *Moringa oleifera* Lam. (Moringaceae) that have a long history of traditional uses as antiviral. *Z. officinalis* is a spice with several pharmacological properties. Chang et al. (2013) reported that fresh ginger reduced human respiratory syncytial virus infection by more than 70 % in human respiratory tract cell lines HEp-2 and 549. A study on *A. annua* has also shown that it has potential as an antiviral agent in the control of flaviruses (Romero et al. 2006), human cytomegalovirus, herpes simplex virus, and hepatitis virus (Efferth et al. 2008). Recently, Nair et al. (2021) showed that *A. annua* extracts could inhibit SARS-CoV-2 replication *in vitro*. *M. oleifera* (also known as "drum stick or horse radish") is well distributed and cultivated in Asia, Africa, Latin America, the Caribbean, and the Pacific Island due to its numerous nutritional and medicinal importance. The antiviral potentials of *M. oleifera* against herpes simplex virus, hepatitis B virus, influenza virus, Epstein–Barr virus, and human immunodeficiency virus have been reported (Biswas et al. 2020). A molecular docking study conducted by Chakotiya and Sharma (2020) showed that shogaol, zingerone, and zingiberene from *Z. officinalis* had higher binding affinities for TMPRSS2 compared to camostat mesylate, a standard TMPRSS2 inhibitor. Laksmiani et al. (2020) also studied the interactions between three phytochemicals from *M. oleifera* (apigenin, luteolin, and quercetin) and TMPRSS2 *via* molecular docking. However, in this current study, molecular docking was performed to analyze the interactions between several phytochemicals from the study plants and TMPRSS2. The stability of the resulting protein-ligand complexes was further assessed by molecular dynamics simulation.

The development of a molecule or compound into a new clinically acceptable drug takes an average of 12 years and cost over $1 billion (Mohs & Greig, 2017). However, the application of computational methods has shortened the period required to detect a compound that could be utilised as a potential clinical candidate (Lin et al. 2020). Interactions between several compounds and protein targets can be studied *in silico* using computer programs to select lead compounds that could be developed into clinical drugs. *In silico* screening of compounds does not only aid the rapid discovery of compounds with therapeutic values but also reduces the cost of developing new drugs. Computational studies also offer the opportunity of determining the ADME (Absorption, Distribution, Metabolism, and Excretion) and "drug-likeness" of promising natural compounds, hence, helping in ruling out compounds that might not be effective during the different steps of drug development (Lombardo et al. 2017). As researchers continue to hunt for arsenals to treat SARS-CoV-2 infection, the *in silico* evaluation of natural plant-derived compounds *via* molecular docking and molecular dynamics simulation can assist in the quick discovery of drugs to treat COVID-19.

Therefore, in this study, compounds from three important medicinal plants (*Z. officinalis, A. annua*, and *M. oleifera*) were screened as potential inhibitors of TMPRSS2, an important protein implicated in the SARS-CoV-2 infection.

Materials and methods

Homology modelling of drug target (TMPRSS2)

The amino acid sequence of TMPRSS2 (Uniprot accession number O15393) comprising 492 amino acids was retrieved from Uniprot database (https://www.uniprot.org/), and then used to predict the protein 3D structure of TMPRSS2 by homology modelling. The amino acid sequence of TMPRSS2 was subjected to BLAST search in the SWISS-MODEL (https://swissmodel.expasy.org/), an automated protein structure homology-modelling server to obtain a template protein structure. The BLAST search returned the crystal structure of serine protease hepsin in complex with inhibitor (SMTL ID 5ce1.1) as the template protein structure for the homology-modelling.

The template protein structure was used to build a homology model of TMPRSS2 using the ProMod3 3.1.1 program of the SWISS-MODEL online server. The model obtained was validated using PROCHECK (https://servicesn.mbi.ucla.edu/PROCHECK/), ERRAT (https://servicesn.mbi.ucla.edu/ERRAT/), and verify3D (https://servicesn.mbi.ucla.edu/Verify3D/).

Identification of active sites and prediction of binding pockets in the TMPRSS2 model

The computed atlas of surface topography of proteins (CASTp) server (http://sts.bioe.uic.edu/) was used to predict the binding pockets of the modelled TMPRSS2, and the distribution of actives sites residues (substrate binding: Asp435, Ser460, and Gly462; catalytic: His296, Asp345, and Ser441) previously reported (Idris et al. 2020) in the pockets.

Table 1
The characteristics of template used in generating TMPRSS2 and quality assessment of TMPRSS2 model generated.

Features of template used in generating TMPRSS2 model	
Template Swiss model ID	5ce1.1A
Sequence Identity	33.33
Resolution	2.5 Å
Sequence similarity	0.38
Coverage	0.71
Template description	Serine protease hepsin
Quality assessment of the TMPRSS2 model generated	
Qualitative Model Energy Analysis (QMEAN)	-1.47
Global Quality Estimation Score (GMQE)	0.49
RSMD	0.148 Å

Phytochemical selection for molecular docking on TMPRSS2 protein model

The SDF files of 2D chemical structures of the 132 phytochemicals were downloaded from the PubChem database (https://pubchem.ncbi.nlm.nih.gov/) and used for the molecular docking. Camostat mesylate, an approved serine inhibitor reported to have promising therapeutic effects against the SARS-CoV-2 virus, served as a control molecule. The compound list is available in Supplementary Material Tables S1-S3.

Molecular docking of phytochemicals on TMPRSS2 protein model

The molecular docking between phytochemicals and modelled 3D structure of transmembrane protease serine 2 (TMPRSS2) was performed using Open babel and Autodock vina wizard on PyRx virtual screening tool. Compound structures (ligand) were minimized and converted to pdbqt format. For this analysis the receptor was treated rigid. The vina search space grid centre selected was X: 13.1910 Y: -6.0318 Z: 15.7311, and was set around reported catalytic (His296, Asp345, and Ser441) and substrate binding (Asp435, Ser460, and Gly462) residues of TMPRSS2 (Idris et al. 2020). The binding affinity (kcal/mol) was obtained after docking. The visualization of the interaction between ligands (compounds) and the TMPRSS2 protein model was done using BIOVIA Discovery studio visualizer 2020 and PyMOL software. The binding affinity obtained for the camostat mesylate, a known inhibitor of TMPRSS2, was set as the cut-off to select compounds for further analysis.

Assessment of drug-likeness and ADMET (absorption, distribution, metabolism, excretion and toxicity) of phytochemicals

The drug-likeness and ADMET properties of compounds predicted to be potential and potent inhibitors of TMPRSS2 were evaluated using the admetSAR web tool (Cheng et al. 2012). The drug-likeness was predicted based on the Lipinski rule of 5 (Benet et al. 2016).

Molecular dynamics simulation

Molecular dynamics simulation was performed using GROMACS version 2018.4 (Abraham et al. 2018). Ligand topologies were generated based on General Amber Force Field (GAFF) using ACPYPE-AnteChamber PYthon Parser interface (Sousa da Silva and Vranken, 2012), and protein topology was generated based on Amber03 using pdb2gmx. The unit cell was defined as a dodecahedron and filled with TIP3P (three-site transferrable intermolecular potential) water. To neutralize the system, six chloride ions (Cl^-) were added. The energy minimization step was performed using the steepest descent minimization with a maximum force $<$ 10.0 kJ/mol. Then, the system was equilibrated in two phases. Firstly, NVT ensembled with 300 K as the reference temperature, and secondly, NPT ensembled with 1 bar as the reference pressure. Both were 100 ps long with a position restraining force on the heavy atoms of the protein and ligand. Once the system was equilibrated, a 50 ns molecular dynamic simulation was run. Analysis of the trajectory was composed by root-mean-square deviation (RMSD) calculation of the heavy atoms of the ligand and an energy decomposition analysis, which was performed using gmx-MMPBSA (Modifed Molecular Mechanics–Poisson Boltzmann Surface Area) with 100 frames from the last 10 ns of each molecular dynamic simulation.

Results and discussion

Homology modelling of TMPRSS2 and model validation

The BLAST search of the amino acid sequence of TMPRSS2 obtained from the Uniprot database against the SWISS-MODEL library generated crystal structure of serine protease hepsin (SMTL ID 5ce1.1). The homology model for TMPRSS2 protein was then built using the crystal structure of serine protease hepsin as a template. The template has a sequence coverage of 71 % and resolution of 2.50 Å. It also shared sequence identity and similarity of 33.33 % and 38 %, respectively, with the query sequence (Table 1). Based on the report of Xiang (2006), the sequence similarity value obtained was suitable to generate a reliable model. The model obtained has a QMEAN (Qualitative Model Energy Analysis) value of -1.47 and global quality estimation score (GMQE) of 0.49 based on the result from ProMod3 3.1.1 in the SWISS-MODEL (Table 1). For biomedical applications, protein models must be accurately predicted. The QMEAN value otherwise, known as “degree of nativeness” indicates, how comparable the model is to the experimental structures. A good model is expected to have a QMEAN value close to zero and not less than -4.0 (Benkert et al. 2011). In the study, the QMEAN score (-1.47) obtained for the predicted protein model confirmed its good quality. The GMQE result is also reliable because the value (0.49) obtained falls between 0 and 1, which is the benchmark, as reported by Biasini et al. (2014). Based on the Ramachandran plot (Fig. 1), the modelled TMPRSS2 has 99.6 % of its residues in the allowed region, 88.6 % in the most favoured region, and 11.0 % in the additional allowed region. This result also supported the good quality of the protein model. The modelled TMPRSS2 was further validated to be of good quality based on the overall quality factor of 95.56 % obtained from ERRAT2 plot analysis (Supplementary Fig. S1).

Identification of active sites and prediction of binding pockets on the TMPRSS2 model

CASTp server predicts topographic characteristics such as cavities, channels, and surface pockets of proteins (Tian et al. 2018). The result of CASTp can reveal the position of active sites such as the binding and catalytic sites of proteins. It can also reveal pockets in which ligand and amino acid residues interaction occur. The CASTp software predicted 75 pockets with the active site residues (His296, Asp345, Asp435, Ser460, and Gly462) with the exception of Ser441 distributed in 10 pockets (Supplementary Fig. S2). The area, volume, and residues around the active sites are presented in Table 2. The Asp435 residue is very important in the TMPRSS2 for substrate binding, recognition, and orientation for the catalytic process, and its presence indicates the trypsin-like proteolytic activity of TMPRSS2 (Vivek-Ananth et al. 2020; Hempel et al. 2021). Therefore, compounds that bind to the Asp435 were taken as the potential inhibitor of TMPRSS2. The Asp435 residue was present in 6 pockets designated 4A, 15B, 25D, 45F, 48G, and 50H. Meanwhile, the catalytic residue Asp345 was present in four pockets (20C, 32E, 51I, and 68J), and His296 in one pocket (32E). However, the ligand-protein interactions were observed to occur in the TMPRSS2 pocket designated 4A, with an area and volume size of 160.709SA and 80.898SA, respectively (Table 2).

Molecular docking of phytochemicals on TMPRSS2 protein model

The result of the molecular docking of 132 phytochemicals selected from three medicinal plants with the TMPRSS2 protein is presented in

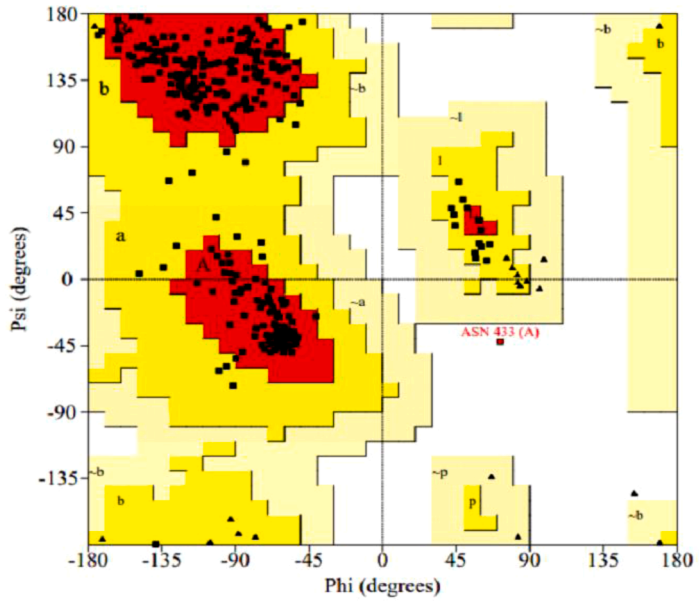

A.

Plot statistics

Residues in most favoured regions [A,B,L]	265	88.6%
Residues in additional allowed regions [a,b,l,p]	33	11.0%
Residues in generously allowed regions [~a,~b,~l,~p]	0	0.0%
Residues in disallowed regions	1	0.3%
Number of non-glycine and non-proline residues	299	100.0%
Number of end-residues (excl. Gly and Pro)	2	
Number of glycine residues (shown as triangles)	29	
Number of proline residues	16	
Total number of residues	346	

Based on an analysis of 118 structures of resolution of at least 2.0 Angstroms and R-factor no greater than 20%, a good quality model would be expected to have over 90% in the most favoured regions.

B.

C.

Fig. 1. Quality check on the TMPRSS2 protein model (A). The PROCHECK Ramachandran plot for the validation of the modelled TMPRSS2 protein. (B). The statistics from the PROCHECK Ramachandran plot. (C). The 3D structure of the modelled TMPRSS2 protein.

the Supplementary Tables S1, S2, and S3.The reference compound camostat mesylate had a binding affinity score of -7.0 kcal/mol. Hence, phytochemicals with binding affinity scores of ≤ -7.0 kcal/mol were selected for further analysis. Twenty (20) phytochemicals had binding affinity scores ≤ -7.0 kcal/mol out of 132 phytochemicals with binding affinity scores ranging from -7.0 to -8.7 kcal/mol. The bond interaction between the compounds and TMPRSS2 residues are presented in Table 3. TMPRSS2 residues Asn398, Asp435, and Gly258 form a strong N−H•••O hydrogen bond type interaction with the control camostat mesylate. (Fig. 2a). The formation of hydrogen bond between a ligand and target protein is important for a molecule's function (Wu et al. 2012). The presence of hydrogen bonds also encourages the formation of stronger and robust ligand-protein complexes (Majewski et al. 2019). However, the numerous van der Waals, covalent, π-alkyl, and electrostatic interactions observed between study compounds and TMPRSS2 can also help in stabilizing the ligand-protein complex.

There was no interaction between TMPRSS2 and two compounds found in *Z. officinalis* (thujopsene and zingiberol) when the docking interaction output was imported into Discovery Studio for visualization. All the compounds with binding energy ≤ -7.0 kcal/mol except gamma-elemene, beta-elemene, and aromadendrene formed hydrogen bonds with residues on TMPRSS2 (Table 4 and Supplementary Fig. S3-S14). However, only five compounds, namely quercetin, glucotropaeolin, niazirin, and moringyne from *M. oleifera*, and scopolin from *A. annua* formed hydrogen bonds with the important substrate binding residue Asp435 (Fig. 2b – f). Our findings established that these five compounds could serve as potential inhibitors of TMPRSS2. Scopolin formed a weak carbon hydrogen (C−H•••O) bond of 3.46 Å in length (L) with the Asp435 residue (Fig. 2b). It also formed the same weak hydrogen bond interaction with residues Gly259 (L= 3.30 Å), Asp440 (L= l3.30 Å and 3.32 Å), and Thr387 (L= 3.65 Å). It interacted with residues Asp440 (L= 2.72 Å), Gly383 (L= 1.83 Å), and Asn398 (L= 1.98 Å) with a strong covalent hydrogen bond (O−H•••O). Other interaction observed between scopolin and TMPRSS2 was a hydrophobic alkyl/π-alkyl bond involving residues Cys465 (L= 3.71 Å), Ala466 (L= 3.93 Å and 5.23 Å), and Cys437 (L= 3.86 Å). Scopolin (the glucoside of the coumarin scopoletin) has different pharmacological properties, such as antioxidant, antimicrobial, anticoagulant, anti-inflammatory, and anticancer properties. It has also been suggested for the treatment of osteoporosis (Park et al. 2020) and obesity (Park et al., 2020), that are two of the risk factors for SARS-CoV-2 infections. Similarly, glucotropaeolin formed a weak carbon-hydrogen bond with residues Asp435 (L= 3.46 Å) and Asp440 (L = 3.06 Å), a strong N−H•••O hydrogen bond type with residue Thr387 (L= 2.57 Å), and a strong O−H•••O hydrogen bond type with Asn398 (L= 2.43 Å), Ala386 (L= 2.48 and 2.49 Å), and Asp440 (L= 2.47 and 3.02 Å). Glucotropaeolin also formed a π-alky bond of length

Table 2
Table showing the area and volume of 10 predicted pockets containing the active (catalytic and binding sites) residues and their surrounding amino acid residues.

Pocket	Area (SA)	Volume (SA)	Amino acid residues present
Pocket 4A	160.709	80.898	Gly259, Ile 381, Ser382, Gly383, Gly385, Ala386, Thr387, Glu388, Asn398, Ala399, Ala400, Asn433, Val434, Asp435*, Ser436, Cys437, Asp440, Gly443, Pro444, Thr 459, Cys465, Ala466
Pocket 15B	37.882	10.655	Asp435*, Ser436, Cys437, Thr459, Trp461, Gly462*, Gly464, Cys465, Gly472, Val473, Tyr474
Pocket 20C	29.858	4.191	Lys342, Asn343, Asn344, Asp345*, Ile346, Ala423, Met424, Asp458, Ser460*, Tyr474, Gly475, Val477, Phe480
Pocket 25D	15.208	2.497	Gly428, Phe429, Gly432, Val434, Asp435*, Ala466, Lys467, Arg470, Pro471
Pocket 32E	6.342	1.113	His296*, Tyr337, Lys342, Asp345*, Ser460*, Trp461
Pocket 45F	2.396	0.107	Asp435* Gly462*, Ser463, Gly464, Arg470, Pro471, Gly472
Pocket 48G	1.339	0.058	Asp435*, Ser463, Gly464, Cys465, Ala466, Lys467, Arg470
Pocket 50H	0.969	0.039	Ile381, Val402, Ala427, Asp435*, Tyr474
Pocket 51I	0.754	0.028	Ala294, Asp345*, Asp458, Ser460*
Pocket 68J	0.029	0.000	Asp345*, Asp458, Ser460*, Gly475

Keys
* = The active site residues.

Table 3
The docking scores for phytochemicals with potential capacity for inhibiting TMPRSS2.

S/N	Plant	Phytochemicals	PubChem ID	Binding energy (kcal/mol)
1.	*Zingiber officinalis*	Thujopsene	442402	-8.7
2.	Roscoe	Zingiberol	5317270	-8.7
3.	(Zingiberaceae)	Gamma-elemene	6432312	-8.1
4.		Beta-elemene	9859094	-8.1
5.		Aromadendrene	11095734	-8.2
6.	*Artemisia annua* L.	Scopolin	439514	-7.3
7.	(Asteraceae)	Lumichrome	5326566	-7.0
8.	*Moringa oleifera* Lam.	Epicatechin	72276	-7.5
9.	(Moringaceae)	Niazirin	129556	-7.1
10.		Glucotropaeolin	656498	-7.2
11.		Quercetin	5280343	-8.0
12.		Apigenin	5280443	-7.4
13.		Luteolin	5280445	-7.9
14.		Rutin	5280805	-7.1
15.		Kaempferol	5280863	-7.3
16.		Isorhamnetin	5281654	-7.0
17.		Myricetin	5281672	-8.3
18.		Astragalin	5282102	-7.8
19.		Marumoside A	101794623	-7.1
20.		Moringyne	131751186	-7.1
21.	Control	Camostat mesylate	5284360	-7.0

5.36 with a residue Val434 of the TMPRSS2 (Fig. 2c). Glucotropaeolin is a glucosinolate, which has been reported to be toxic and antinutritive (Al-Gendy et al. 2016).

Quercetin formed a strong hydrogen bond (O−H•••O) with residues Asp435 (L= 2.46 Å), Gly385 (L= 2.37 Å), Gly383 (L= 2.21 Å), Asn398 (L= 3.02 Å), and Asn433 (L= 2.81 Å) (Fig. 2d), while niazirin formed a similar bond with residues Asp435 (L= 2.78 and 3.00 Å) and Asn433 (L= 1.82 and 1.98 Å) (Fig. 2e). A weak carbon-hydrogen (was formed between quercetin and Asp398 (L = 3.35 Å) and Gly259 (L= 3.44 Å) residues of TMPRSS2. A similar interaction was also observed between niazirin and the Gly259 (L= 3.29 Å) residue. Both compounds bind with the Ala400 residue of the TMPRSS2 through a π-alkyl bond of length 4.70 Å and 4.80 Å for quercetin and niazirin, respectively. Moringyne binds to six residues of the TMPRSS2 via a strong hydrogen bond (O−H•••O). These residues include Asp435 (L= 2.44 Å), Asp440 (L= 3.06 Å), Gly383 (L= 2.26 Å), Asn398 (L= 2.04 and 2.52 Å), and Gly385 (L= 2.41 Å). A weak hydrogen bond was observed between moringyne and two TMPRSS2 residues, including Ala434 (L= 3.48 Å) and Asp440 (L= 3.19 Å). It also binds to the Ala 466 residue via a π-alkyl bond of length 4.63 Å (Fig. 2f). Moringyne is a glycoside reported to relax bronchioles, and hence, it is used in the treatment of asthma (Mahajan et al. 2009). Due to this property, it could be very useful as an adjuvant for the treatment of COVID-19 infections, which produce severe breathing difficulties.

According to Jeffrey (1997), hydrogen bond with distances ranging between 2.2 – 2.5 Å is classified as strong covalent hydrogen bond, while moderate and weak electrostatic hydrogen bond have distances ranging between 2.5 – 3.2 Å and 3.2 – 4.0 Å respectively. Therefore, based on interaction with the binding substrate Asp435 and hydrogen bonding, all the biologically active constituents derived from *M. oleifera* (quercetin, niazirin, and moringyne) could serve as potent inhibitor of TMPRSS2 among all the biological compounds tested.

Assessment of drug-likeness and ADMET of phytochemicals

According to the Lipinski rule of five, a small compound that has the potential to become a drug must have certain properties. The compound must have molecular weight less than 500, the hydrogen bond donor (H-Bond donor), and hydrogen bond acceptor (H-Bond acceptor) must not be more than 5 and 10 respectively. The calculated Log P (CLog P), which is the octanol–water partition coefficient logP, must not be more than 5 (Benet et al. 2016). All the compounds, including the control, did not violate any of the Lipinski rules of five (Table 5), and as such, they possess drug-like features. Studies on the pharmacokinetics and toxicity of potential drug molecules are essential. The three phytochemicals (niazirin, quercetin, and moringyne) exhibited the highest potential to inhibit TMPRSS2 based on the molecular docking result, exhibiting different ADMET properties (Table 6). The control compound camostat mesylate has good human intestinal absorption (HIA), blood brain barrier (BBB), and human oral bioavailability (HOB) properties. It is not carcinogenic, according to AMES mutagenesis prediction, and has acute oral toxicity of level III i.e. it has a lethal dose 50 (LD_{50}) that is less than 500 but greater than 5000 mg/kg (Ammar, 2017). However, camostat mesylate is hepatotoxic according to the admetSAR server prediction. It was also found in this study that quercetin and moringyne can be absorbed in the intestine, and none of the compounds including niazirin can cross the blood brain barrier. Contrarily, accumulation of quercetin in rat brain tissues has been reported (Ishisaka et al. 2011). The admetSAR program predicted the compounds as non-carcinogenic and not orally bioavailable. However, several approaches such as absorption enhancer (Aungst, 2012), chemical modification (Renukuntla et al. 2013), and self-double-emulsifying drug delivery system (Wang et al. 2017) methods can be used to improve the oral bioavailability of the compounds. According to the AMES test, quercetin was predicted as a mutagen with a probability of 0.9000. It has level II acute oral toxicity. This implies that the LD_{50}, which is the amount of compound or drug required to kill 50 % of the animals on which it is being tested, is greater than 50 but less than 500 mg/kg (Ammar, 2017). Quercetin was also

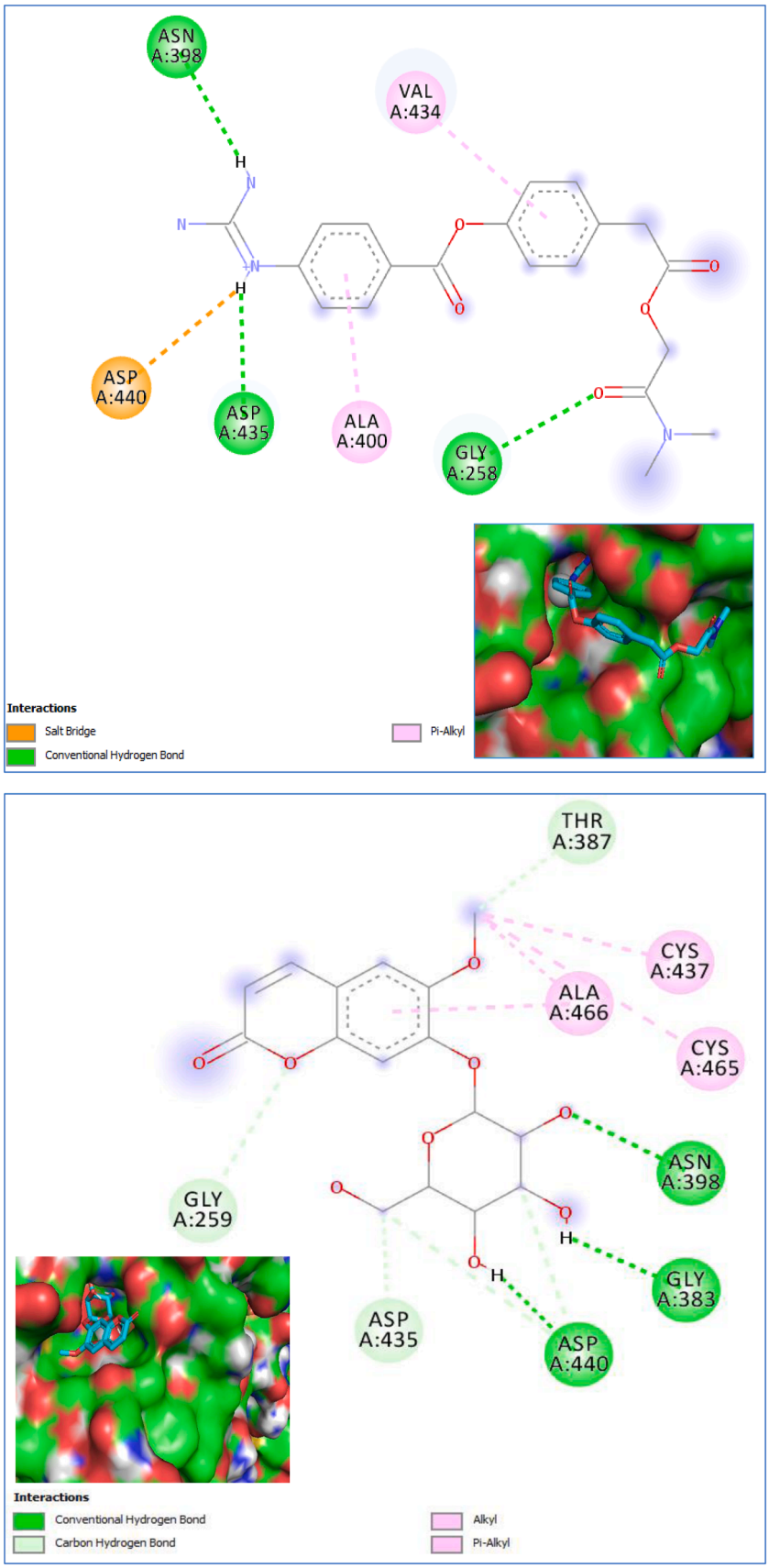

Fig. 2. a-f. The ligand-protein interaction between TMPRSS2 and (a). Camostat mesylate (b). Scopolin (c). Glucotropaeolin (d). Quercetin (e). Niazirin (f). Moringyne. The images show the binding of the phytochemicals on the TMPRSS2 pocket (inset).

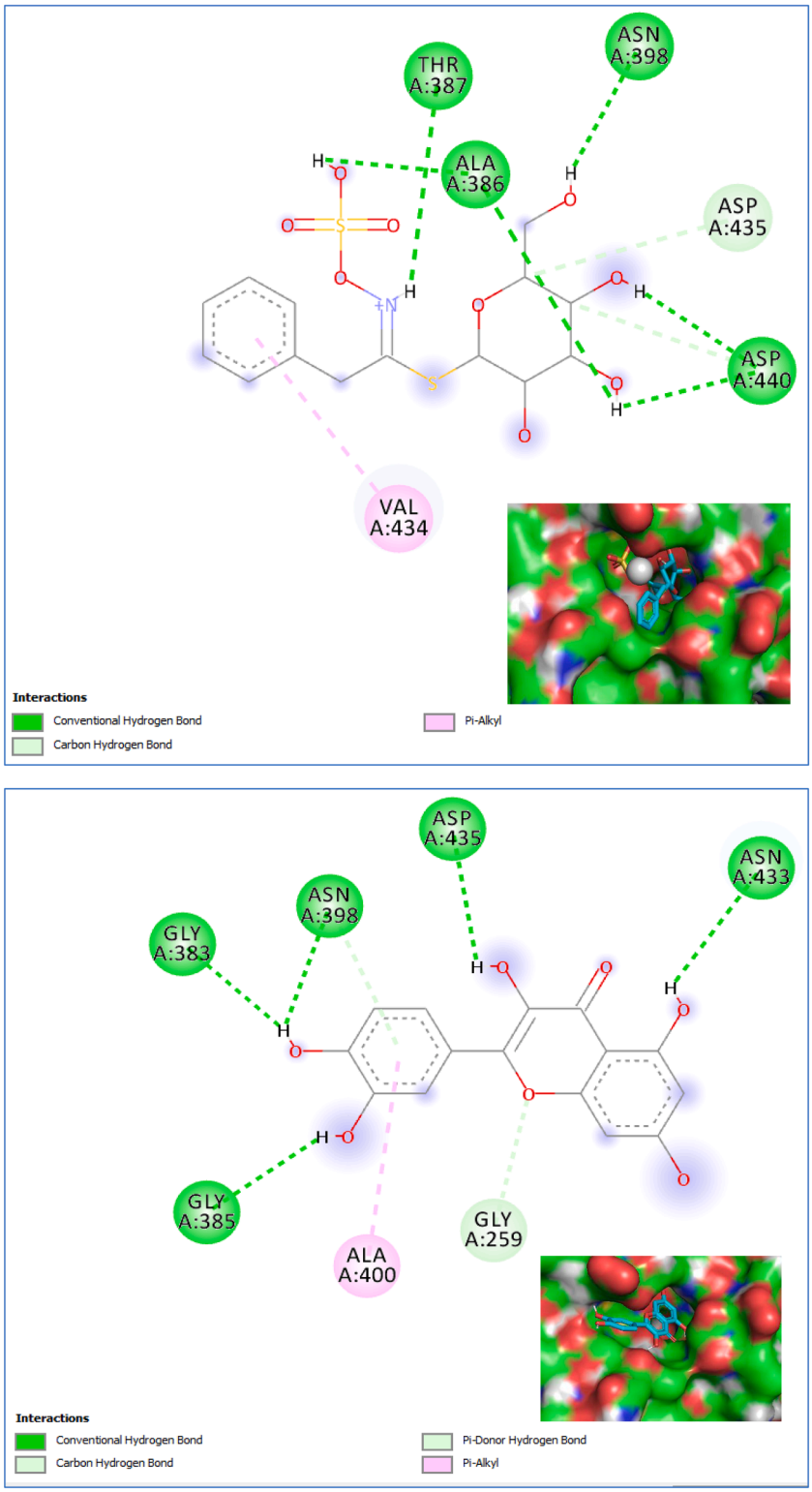

Fig. 2. (*continued*).

predicted as a hepatotoxic compound. Based on the AMES, acute oral toxicity, and hepatotoxicity test results of quercetin, there is a need to apply caution in its application as a potential TMPRSS2 inhibitor. This result corroborates the findings of Ammar (2017). There is a dearth of information about the pharmacokinetics and toxicity of moringyne, and further research on this compound might lead to the development of an excellent lead compound for the treatment of SARS-CoV-2 infection.

Molecular dynamics simulation

As shown in Fig. 3a, the reference compound camostat mesylate in complex with TMPRSS2 showed a trajectory with a clear fluctuation from 5 to 30 ns, but after this time, the system stabilizes around 5 Å. In the case of quercetin, the RMSD never reached a stable state, and at 30 ns, the ligand moved away from the protein, therefore, causing a drastic reduction in the RMSD value. In contrast to niazirin and moringyne, lack

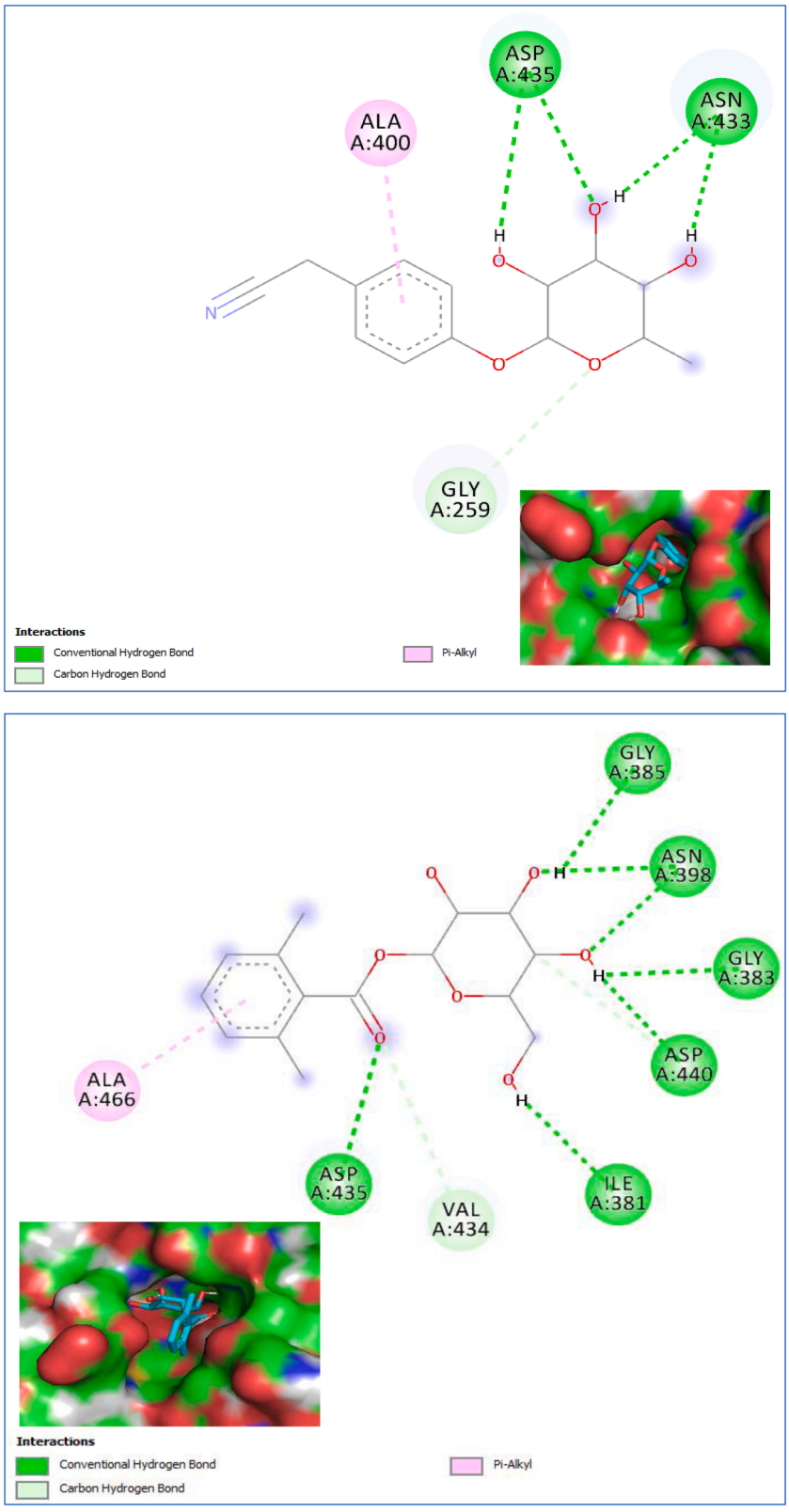

Fig. 2. (*continued*).

of sugar moeity in the quercetin can affect its flexibility and stability because the sugar ring and the rotation of the glycosidic bond can generate several sites of interactions. The relative frequency of molecular interactions in the last 10 ns of simulation from camostat mesylate, niazirin, and moringyne trajectories suggests that Asp440, Ser436, and Gly385 have significant contributions to the ligand binding because the three compounds bind to these residues primarily by hydrogen bonding (Fig. 3b). From the RMSD result, camostat mesylate is a highly flexible compound, therefore interacts at a low relative frequency, except for its hydrogen bond interaction with Asp440, Ser436, and Gly385. On the

Table 4
The bond interactions between the potential phytochemical inhibitors with binding affinities ≤ -7.0 kcal/mol and TMPRSS2.

Compound	Interaction between compounds and TMPRSS2 protein residues								
	Hydrogen Bond	Carbon-hydrogen bond/π-Donor hydrogen Bond	Alky/π-Alky bond	Salt bridge	π-Anion	π-Sigma	π-Sulfur	π-Lone Pair	Unfavourable Donor-Donor/Acceptor-Acceptor
Camostat mesylate	Asn398, **Asp435**, Gly258	-	Val434, Ala400	Asp440	-	-	-	-	-
Beta- and Gamma-elemene	-	-	Ala400, Ile381	-	-	-	-	-	-
Aromadendrene	-	-	Ala400, Ile381	-	-	-	-	-	-
Scopolin	Asn398, Gly383, Asp440	Thr387, **Asp435**, Gly259	Ala466, Cys437, Cys465	-	-	-	-	-	-
Lumichrome	Asp440, Asn398	-	Ala400, Ile381	-	-	-	-	-	Asn398
Myricetin	Asn433, Ile381, Asp440,	Asn398, Gly259	Ala400	-	-	-	-	-	-
Quercetin	Asn433, Asn398, Gly385, Gly383, **Asp435**	Gly259, Asn398	Ala400	-	-	-	-	-	-
Luteolin	Asp440	Asn398	Ala400, Ala466	-	-	Ala466	Cys437	Thr387	Gly383
Astragalin	Asp440	Gly259	Val434, Cys465	-	-	Glu388, Ala466, Gly259	Cys437	-	-
Epicatechin	Asn398, Gly385	Asn398	Ala400, Cys465	-	Asp440	Ala466	Cys437	Thr387	Glu389
Apigenin	Gly383, Ile381		Val434, Ala400	-	Asp440	-	-	-	-
Kaemferol	Gly383	Gly259, Asn398	Ala400	-	-	-	-	-	-
Glucotropaeolin	Asp440, Asn398, Thr387, Ala386	**Asp435**, Asp440	Val434	-	-	-	-	-	-
Niazirin	Asn433, **Asp435**	Gly259	Ala400	-	-	-	-	-	-
Rutin	Gly259, Gly385, Ala386	Gly258	Lys401, Val434, Ala400, Cys465	-	-	Ala466, Glu388	-	Thr387	Glu389
Marumoside A	Gly383, Gly385	Gly259	Ala400, Ile381, Val434	-	-	-	-	-	Ala386
Moringyne	Ile381, Asp440, Asn398, Gly385, Gly383, **Asp435**,	Val434	Ala466	-	-	-	-	-	-
Isorhamnetin	Asp440	Ile381, Gly259, Asn398	Ala400	-	-	-	-	-	-

Table 5
The molecular and drug-likeness properties of three phytochemicals predicted as potential inhibitors of TMPRSS2.

Compound	Chemical formular	Molecular weight (g/mol)	Saturation (Csp3)	Flexibilty (no of rotatable bond)	Lipophilicity (XLOGP3)	Solubility (log S)	Polarity; TPSA(Å^2)	Molar Refractivity	HBA	HBD
Niazirin	$C_{14}H_{17}NO_5$	279.29	0.50	3	-0.37	-1.36	102.94	68.95	6	3
Quercetin	$C_{15}H_{10}O_7$	302.24	0.00	1	1.54	-3.16	131.36	78.03	7	5
Moringyne	$C_{15}H_{20}O_7$	312.32	0.53	4	0.37	-1.95	116.45	75.31	7	4
Camostat mesylate (control)	$C_{21}H_{26}N_4O_8S$	494.52	0.24	10	0.24	-2.66	200.06	123.31	9	3

Table 6
The ADMET properties of the three phytochemicals predicted as potential inhibitors of TMPRSS2.

Compound	Human Intestinal Absorption (probability)	Blood Brain Barrier (probability)	Human oral bioavailability (probability)	Carcinogenicity (probability)	Ames mutagenesis (probability)	Acute Oral Toxicity (probability)	Hepatotoxicity (probability)
Niazirin	- (0.8428)	- (0.2350)	- (0.5714)	- (0.9714)	- (0.6400)	III (0.7567; LD_{50}>500<5000 mg/kg)	- (0.5250)
Quercetin	+ (0.9833)	- (0.4632)	- (0.5429)	- (1.0000)	+ (0.9000)	II (0.7348; LD_{50}>50<500 mg/kg)	+ (0.7500)
Moringyne	+ (0.7386)	- (0.6538)	- (0.7571)	- (0.9429)	- (0.6900)	III (0.7123; LD_{50}>50<5000 mg/kg)	- (0.6000)
Camostat mesylate (control)	+ (0.8580)	+ (0.9731)	+ (0.5714)	- (0.6499)	- (0.6000)	III (0.5937; LD_{50}>500<5000 mg/kg)	+ (0.8000)

- (negative); + (positive); LD_{50}: Lethal Dose 50.

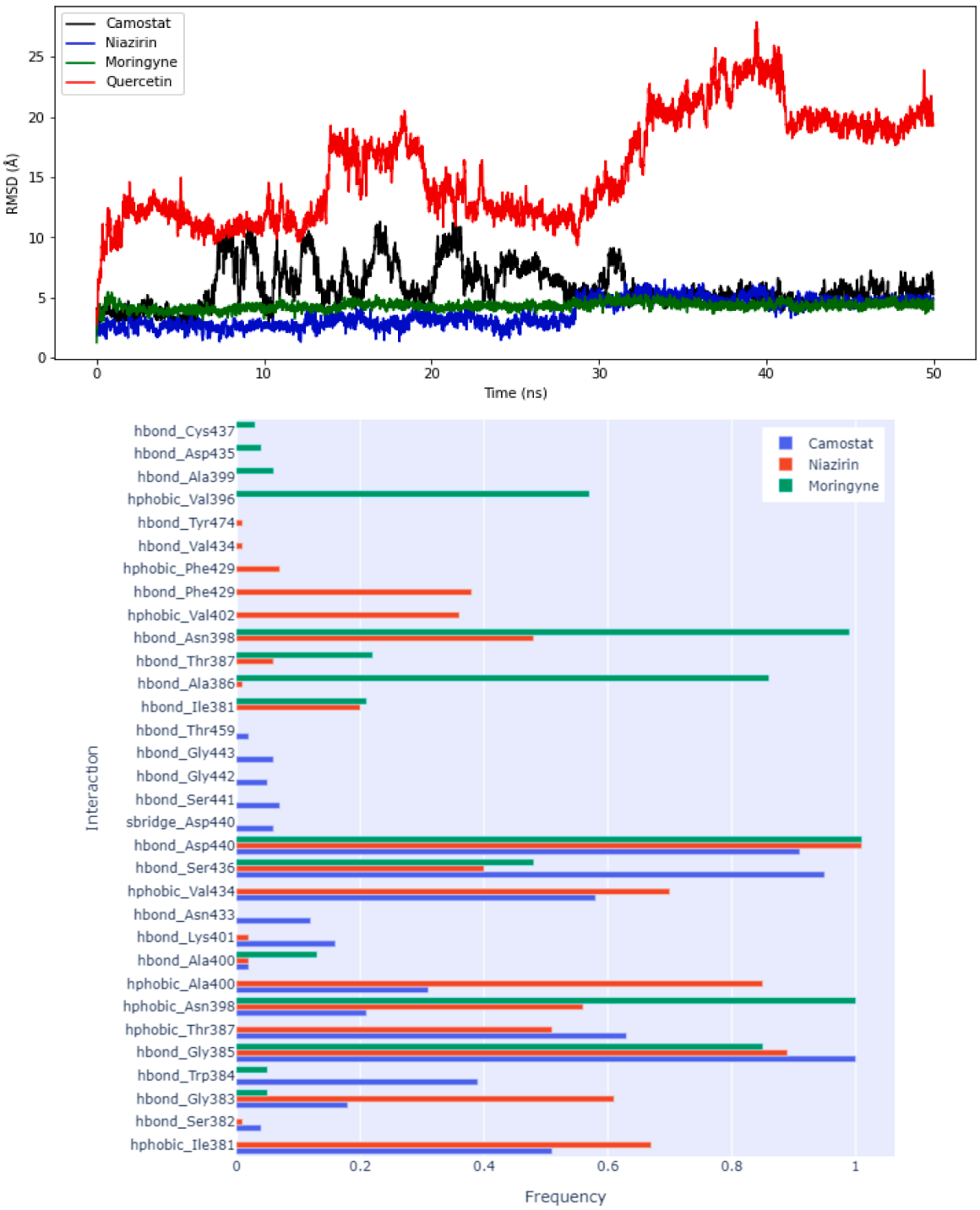

Fig. 3. Molecular dynamics simulation of three phytochemicals and reference drug on TMPRSS2. (a) Heavy-atom RMSD of each compound. (b) Relative frequency of the molecular interactions calculated in the last 10 ns of the molecular dynamic simulation.

other hand, Ile381, Ala400, and Val434 contributed to the stability of niazirin by hydrophobic interactions. The most stable compound, moringyne, forms two additional hydrogen bonds with Ala386 and Asn398, in accordance with the docking pose.

Conclusion

Using computer-aided *in silico* analysis which include homology modelling, molecular docking, and molecular dynamics simulation, we identified three compounds from *M. oleifera*- niazirin, quercetin, and moringyne that can inhibit the activity of human TMPRSS2. The three compounds exhibited satisfactory ADMET properties, though the application of quercetin requires caution. Comparatively, the result of the molecular dynamics simulation suggested moringyne as the best phytochemical to be considered as a potential inhibitor of TMPRSS2. Further experimental studies on niazirin, quercetin, and moringyne are required to consider their application in the treatment and management of SARS-CoV-2 infection.

Declaration of Competing Interest

The authors declare that there are no known conflicts of interest

associated with this publication and there has been no significant financial support for this work that could have influenced its outcome.

Supplementary materials

Supplementary material associated with this article can be found, in the online version, at doi:10.1016/j.phyplu.2021.100135.

References

Abraham, M.J., Van Der Spoel, D., Lindahl, E., Hess, B., the GROMACS development team, 2018. GROMACS user manual version 2018.1. www.gromacs.org.

Al-Gendy, A.A., Nematallah, K.A., Zaghloul, S.S., Ayoub, N.A., 2016. Glucosinolates profile, volatile constituents, antimicrobial, and cytotoxic activities of *Lobularia libyca*. Pharm. Biol. 54, 3257–3263. https://doi.org/10.1080/13880209.2016.1223146 https://doi.org/.

Ammar, O., 2017. *In silico* pharmacodynamics, toxicity profile and biological activities of the Saharan medicinal plant *Limoniastrum feei*. Brazilian J. Pharm. Sci. 53 https://doi.org/10.1590/s2175-97902017000300061 https://doi.org/.

Aungst, B.J., 2012. Absorption enhancers: applications and advances. AAPS J. 14, 10–18. https://doi.org/10.1208/s12248-011-9307-4 https://doi.org/.

Benet, L.Z., Hosey, C.M., Ursu, O., Oprea, T.I., 2016. BDDCS, the rule of 5 and drugability. Adv. Drug Deliv. Rev. 101, 89–98. https://doi.org/10.1016/j.addr.2016.05.007 https://doi.org/.

Benkert, P., Biasini, M., Schwede, T., 2011. Toward the estimation of the absolute quality of individual protein structure models. Bioinformatics 27, 343–350. https://doi.org/10.1093/bioinformatics/btq662 https://doi.org/.

Biasini, M., Bienert, S., Waterhouse, A., Arnold, K., Studer, G., Schmidt, T., Kiefer, F., Cassarino, T.G., Bertoni, M., Bordoli, L., Schwede, T., 2014. SWISS-MODEL: modelling protein tertiary and quaternary structure using evolutionary information. Nucleic Acids Res 42, W252–W258. https://doi.org/10.1093/nar/gku340 https://doi.org/.

Biswas, D., Nandy, S., Mukherjee, A., Pandey, D.K., Dey, A., 2020. *Moringa oleifera* Lam. and derived phytochemicals as promising antiviral agents: A review. S. Afr. J. Bot. 129, 272–282. https://doi.org/10.1016/j.sajb.2019.07.049 https://doi.org/.

Chakotiya, A.S., Sharma, R.K., 2020. Phytoconstituents of *zingiber officinale* targeting host-viral protein interaction at entry point of sars-COV-2: A molecular docking study. Def. Life Sci. J. 268–277. https://doi.org/10.14429/dlsj.5.15718 https://doi.org/.

Chang, J.S., Wang, K.C., Yeh, C.F., Shieh, D.E., Chiang, L.C., 2013. Fresh ginger (*Zingiber officinale*) has anti-viral activity against human respiratory syncytial virus in human respiratory tract cell lines. J. Ethnopharmacol. 145, 146–151. https://doi.org/10.1016/j.jep.2012.10.043 https://doi.org/.

Cheng, F., Li, W., Zhou, Y., Shen, J., Wu, Z., Liu, G., Lee, P.W., Tang, Y., 2012. admetSAR: a comprehensive source and free tool for assessment of chemical ADMET properties. J. Chem. Inf. Model. 3099–3105. https://doi.org/10.1021/ci300367a https://doi.org/.

Efferth, T., Romero, M.R., Wolf, D.G., Stamminger, T., Marin, J.J., Marschall, M., 2008. The antiviral activities of artemisinin and artesunate. Clin. Infect. Dis. 47, 804–811. https://doi.org/10.1086/591195 https://doi.org/.

Hempel, T., Raich, L., Olsson, S., Azouz, N.P., Klingler, A.M., Hoffmann, M., Pöhlmann, S., Rothenberg, M.E., Noé, F., 2021. Molecular mechanism of inhibiting the SARS-CoV-2 cell entry facilitator TMPRSS2 with camostat and nafamostat. Chem. Sci. 12, 983–992. https://doi.org/10.1039/d0sc05064d http://doi.org/.

Hoffmann, M., Kleine-Weber, H., Schroeder, S., Krüger, N., Herrler, T., Erichsen, S., Schiergens, T.S., Herrler, G., Wu, N.H., Nitsche, A., Müller, M.A., 2020. SARS-CoV-2 cell entry depends on ACE2 and TMPRSS2 and is blocked by a clinically proven protease inhibitor. Cell 181, 271–280. https://doi.org/10.1016/j.cell.2020.02.052 http://doi.org/.

Idris, M.O., Yekeen, A.A., Alakanse, O.S., Durojaye, O.A., 2020. Computer-aided screening for potential TMPRSS2 inhibitors: a combination of pharmacophore modeling, molecular docking and molecular dynamics simulation approaches. J. Biomol. Struct. Dyn. 1–19. https://doi.org/10.1080/07391102.2020.1792346 https://doi.org/.

Ishisaka, A., Ichikawa, S., Sakakibara, H., Piskula, M.K., Nakamura, T., Kato, Y., Ito, M., Miyamoto, K.I., Tsuji, A., Kawai, Y., Terao, J., 2011. Accumulation of orally administered quercetin in brain tissue and its antioxidative effects in rats. Free Radic. Biol. Med. 51, 1329–1336. https://doi.org/10.1016/j.freeradbiomed.2011.06.017 https://doi.org/.

Jeffrey, G.A., 1997. An Introduction to Hydrogen Bonding, 12. Oxford university press, New York, p. 228.

Laksmiani, N.P.L., Larasanty, L.P.F., Santika, A.A.G.J., Prayoga, P.A.A., Dewi, A.A.I.K., Dewi, N.P.A.K., 2020. Active compounds activity from the medicinal plants against SARS-CoV-2 using *in silico* assay. Biomed. Pharmacol. J. 13, 873–881. https://doi.org/10.13005/bpj/1953 https://doi.org/.

Lin, X., Li, X., Lin, X., 2020. A review on applications of computational methods in drug screening and design. Molecules 25, 1375. https://doi.org/10.3390/molecules25061375 https://doi.org/.

Lombardo, F., Desai, P.V., Arimoto, R., Desino, K.E., Fischer, H., Keefer, C.E., Petersson, C., Winiwarter, S., Broccatelli, F., 2017. *In Silico* absorption, distribution, metabolism, excretion, and pharmacokinetics (ADME-PK): utility and best practices. An industry perspective from the international consortium for innovation through quality in pharmaceutical development. J. Med. Chem. 60, 9097–9113. https://doi.org/10.1021/acs.jmedchem.7b00487 https://doi.org/.

Mahajan, S.G., Banerjee, A., Chauhan, B.F., Padh, H., Nivsarkar, M., Mehta, A.A., 2009. Inhibitory effect of n-butanol fraction of *Moringa oleifera* Lam. seeds on ovalbumin-induced airway inflammation in a guinea pig model of asthma. Int. J. Toxicol. 28, 519–527. https://doi.org/10.1177/1091581809345165 https://doi.org/.

Majewski, M., Ruiz-Carmona, S., Barril, X., 2019. An investigation of structural stability in protein-ligand complexes reveals the balance between order and disorder. Commun. Chem. 2, 1–8. https://doi.org/10.1038/s42004-019-0205-5 https://doi.org/.

McKee, D.L., Sternberg, A., Stange, U., Laufer, S., Naujokat, C., 2020. Candidate drugs against SARS-CoV-2 and COVID-19. Pharmacol. Res., 104859 https://doi.org/10.1016/j.phrs.2020.104859 https://doi.org/.

Mohs, R.C., Greig, N.H., 2017. Drug discovery and development: Role of basic biological research. Alzheimer's Dement.: Transl. Res. Clin. Interv. 3, 651–657. https://doi.org/10.1016/j.trci.2017.10.005 https://doi.org/.

Nair, M.S., Huang, Y., Fidock, D.A., Polyak, S.J., Wagoner, J., Towler, M.J., Weathers, P.J., 2021. *Artemisia annua* L. extracts inhibit the *in vitro* replication of SARS-CoV-2 and two of its variants. J. Ethnopharmacol. 274, 114016 https://doi.org/10.1016/j.jep.2021.114016 https://doi.org/.

Pandey, P., Rane, J.S., Chatterjee, A., Kumar, A., Khan, R., Prakash, A., Ray, S., 2020. Targeting SARS-CoV-2 spike protein of COVID-19 with naturally occurring phytochemicals: an in silico study for drug development. J Biomol Struct Dyn 1–11. https://doi.org/10.1080/07391102.2020.1796811 https://doi.org/.

Park, E., Kim, J., Jin, H.S., Choi, C.W., Choi, T.H., Choi, S., Huh, D., Jeong, S.Y., 2020. Scopolin attenuates osteoporotic bone loss in ovariectomized Mice. Nutrients 12, 3565. https://doi.org/10.3390/nu12113565 https://doi.org/.

Park, E., Lee, C.G., Kim, J., Lim, E., Yeo, S., Jeong, S.Y., 2020. Scopolin prevents adipocyte differentiation in 3T3-L1 preadipocytes and weight gain in an ovariectomy-induced obese mouse. Model. Int. J. Mol. Sci. 21, 8699. https://doi.org/10.3390/ijms21228699 https://doi.org/.

Pooja, M., Reddy, G.J., Hema, K., Dodoala, S., Koganti, B., 2021. Unravelling high-affinity binding compounds towards transmembrane protease serine 2 enzyme in treating SARS-CoV-2 infection using molecular modelling and docking studies. Eur. J. pharmacol. 890, 173688 https://doi.org/10.1016/j.ejphar.2020.173688 https://doi.org/.

Renukuntla, J., Vadlapudi, A.D., Patel, A., Boddu, S.H., Mitra, A.K., 2013. Approaches for enhancing oral bioavailability of peptides and proteins. Int. J. Pharm. 447, 75–93. https://doi.org/10.1016/j.ijpharm.2013.02.030 https://doi.org/.

Romero, M.R., Serrano, M.A., Vallejo, M., Efferth, T., Alvarez, M., Marin, J.J., 2006. Antiviral effect of artemisinin from *Artemisia annua* against a model member of the Flaviviridae family, the bovine viral diarrhoea virus (BVDV). Planta Med 72, 1169–1174. https://doi.org/10.1055/s-2006-947198 https://doi.org/.

Sousa da Silva, A.W., Vranken, W.F., 2012. ACPYPE - antechamber python parser interfacE. BMC Res. Notes 5, 367. https://doi.org/10.1186/1756-0500-5-367. –367https://doi:

Tian, W., Chen, C., Lei, X., Zhao, J., Liang, J., 2018. CASTp 3.0: computed atlas of surface topography of proteins. Nucleic Acids Res 46, W363–W367. https://doi.org/10.1093/nar/gky473 https://doi.org/.

Vivek-Ananth, R.P., Rana, A., Rajan, N., Biswal, H.S., Samal, A., 2020. *In silico* identification of potential natural product inhibitors of human proteases key to SARS-CoV-2 infection. Molecules 25, 3822. https://doi.org/10.3390/molecules25173822 https://doi.org/.

Wang, Q., Hu, C., Qian, A., Liu, T., Zhang, H., Zhang, Y., Xia, Q., 2017. Enhanced oral bioavailability of quercetin by a new non-aqueous self-double-emulsifying drug delivery system. Eur. J. Lipid Sci. Technol. 119, 1600167 https://doi.org/10.1002/ejlt.201600167 https://doi.org/.

Wu, M.Y., Dai, D.Q., Yan, H., 2012. PRL-dock: Protein-ligand docking based on hydrogen bond matching and probabilistic relaxation labeling. Proteins 80, 2137–2153. https://doi.org/10.1002/prot.24104 https://doi.org/.

Xiang, Z., 2006. Advances in homology protein structure modeling. Curr. Protein Pept. Sci. 7, 217–227. https://doi.org/10.2174/138920306777452312 https://doi.org/.

Yadav, P.K., Jaiswal, A., Singh, R.K., 2021. *In silico* study on spice-derived antiviral phytochemicals against SARS-CoV-2 TMPRSS2 target. J. Biomol. Struct. Dyn. 1–11. https://doi.org/10.1080/07391102.2021.1965658 https://doi.org/.